PERGAMON

Chemical Engineering Science 56 (2001) 6863–6871

Chemical Engineering Science

www.elsevier.com/locate/ces

Slow motion of a droplet between two parallel plane walls

Huan J. Keh *, Po Y. Chen

Department of Chemical Engineering, National Taiwan University, Taipei 106-17, Taiwan, ROC

Abstract

A combined analytical–numerical study for the creeping flow caused by a fluid sphere translating in a second, immiscible fluid parallel to two flat plates at an arbitrary position between them is presented. To solve the Stokes equations for the fluid velocity fields inside and outside the spherical droplet, a general solution is constructed from fundamental solutions in both rectangular and spherical coordinate systems. Boundary conditions are enforced first at the plane walls by the Fourier transforms and then on the droplet surface by a collocation technique. Numerical results for the hydrodynamic drag force acting on the droplet are obtained with good convergence for various relative viscosities of the droplet and separation distances between the droplet and the walls. For the motion of a solid sphere (droplet with infinite viscosity) parallel to a single plane wall or to two walls, our drag results are in perfect agreement with the available solutions in the literature for all particle-to-wall spacings. The boundary-corrected drag force exerted on the droplet normalized by the value in the absence of the walls is found to increase monotonically with an increase in the internal-to-external viscosity ratio for any given geometry. © 2001 Published by Elsevier Science Ltd.

Keywords: Creeping flow; Fluid droplet; Drag force; Boundary effect

1. Introduction

The motion of droplets of one fluid dispersed in a second, immiscible fluid plays an important role in a variety of natural and industrial processes, such as raindrop formation, the mechanics and rheology of emulsions, liquid–liquid extraction, and sedimentation phenomena. The creeping-flow translation of a single spherical droplet of radius a in an unbounded medium of viscosity η was first analyzed independently by Hadamard (1911) and Rybczynski (1911). Assuming continuous velocity and continuous tangential shearing stress across the interface between the fluid phases in the absence of surface active agents, they found that the force exerted on the fluid sphere by the surrounding fluid is

$$\mathbf{F}_0 = -6\pi\eta a\frac{3\eta^* + 2}{3\eta^* + 3}\mathbf{U}. \quad (1)$$

Here, $\mathbf{U}$ is the migration velocity of the droplet and η^* is the internal-to-external viscosity ratio. Since the fluid properties are arbitrary, Eq. (1) degenerates to the case of motion of a solid sphere (Stokes' law) when the viscosity of the droplet becomes infinite and to the case of motion of a gas bubble when the viscosity approaches zero.

During the translation of a fluid sphere in a second, immiscible fluid, the interfacial stresses acting at the droplet surface tend to deform it. If the motion is sufficiently slow or the droplet is sufficiently small, the droplet will in the first approximation be spherical. The problems associated with the shape of a droplet undergoing distortion, when inertial effects are no longer negligible, were discussed in the literature (Taylor & Acrivos, 1964; Dandy & Leal, 1989).

In many practical applications of low-Reynolds-number motion, droplets are not isolated and the surrounding fluid is externally bounded by solid walls. Thus, it is important to determine if the presence of neighboring boundaries significantly affects the movement of a droplet. Using spherical bipolar coordinates, Bart (1968) and Rushton and Davies (1973) examined the motion of a spherical droplet settling normal to a plane interface between two immiscible viscous fluids. This work is an extension of the analyses of Maude (1961) and Brenner (1961), who independently analyzed the fluid motion generated by a rigid sphere moving perpendicular to a solid plane surface or to a free surface plane. Wacholder & Weihs (1972) also utilized bipolar coordinates to study the motion of a fluid sphere through another fluid normal to a rigid or free plane surface; their calculations agree with the results obtained by Bart (1968) in these limits.

* Corresponding author. Fax: + 886-2-2362-3040.
E-mail address: huan@ccms.ntu.edu.tw (H. J. Keh).

0009-2509/01/$ - see front matter
PII: S0009-2509(01)00323-2

Hetsroni, Haber, and Wacholder (1970) used a method of reflections to solve for the terminal settling velocity of a spherical droplet moving axially at an arbitrary radial location within a long circular tube filled with a viscous fluid. The wall effects experienced by a fluid sphere moving along the axis of a circular tube were also examined by using the reciprocal theorem (Brenner, 1971) and an approximate approach (Coutanceau & Thizon, 1981).

The parallel motion of a droplet in a quiescent fluid at any position between two parallel flat plates was studied by Shapira and Haber (1988) using the method of reflections. Approximate solutions for the hydrodynamic drag force exerted on the droplet were obtained to the first order of $a/(b+c)$, where b and c are the respective distances from the droplet center to the two plates. Obviously, this result cannot be sufficiently accurate when the value of $a/(b+c)$ is large, say, > 0.2. The purpose of this article is to obtain an exact solution for the slow motion of a spherical droplet parallel to two plane walls at an arbitrary position between them. The creeping-flow equations applicable to the system are solved by using a combined analytical-numerical method with a boundary collocation technique (Ganatos, Pfeffer, & Weinbaum, 1980), and the wall-corrected drag force acting on the droplet is obtained with good convergence for various cases. For the special case of movement of a droplet with infinite viscosity, our calculations show excellent agreement with the available solutions in the literature for the corresponding motion of a solid sphere.

2. Analysis

We consider the steady creeping motion caused by a spherical droplet of radius a translating with a constant velocity $\mathbf{U} = U\mathbf{e}_x$ in an immiscible fluid parallel to two infinite plane walls whose distances from the center of the droplet are b and c, as shown in Fig. 1. Here (x, y, z), (ρ, ϕ, z), and (r, θ, ϕ) denote the rectangular, circular cylindrical, and spherical coordinate systems, respectively, with the origin of coordinates at the droplet center, and $\mathbf{e}_x$ is the unit vector in the x direction. We set $b \leqslant c$ throughout this work, without the loss of generality. The droplet is assumed to be sufficiently small so that interfacial tension (which is assumed to be fairly large) maintains its spherical shape. The fluid is at rest far away from the droplet. The objective is to determine the correction to Eq. (1) for the motion of the droplet due to the presence of the plane walls.

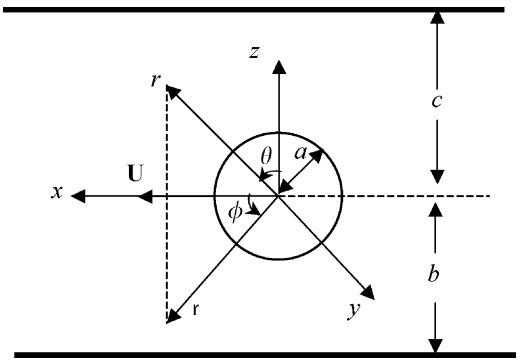

Fig. 1. Geometric sketch of the translation of a spherical droplet parallel to two plane walls at an arbitrary position between them.

The fluids inside and outside the droplet are assumed to be incompressible and Newtonian. Owing to the low Reynolds number, the fluid motion is governed by the Stokes equations,

$$\eta\nabla^2\mathbf{v} - \nabla p = \mathbf{0}, \tag{2a}$$

$$\nabla\cdot\mathbf{v} = 0 \quad (r \geqslant a), \tag{2b}$$

$$\eta_1\nabla^2\mathbf{v}_1 - \nabla p_1 = \mathbf{0}, \tag{3a}$$

$$\nabla\cdot\mathbf{v}_1 = 0 \quad (r \leqslant a), \tag{3b}$$

where $\mathbf{v}_1$ and $\mathbf{v}$ are the fluid velocity fields for the flow inside the droplet and for the external flow, respectively, p_1 and p are the corresponding dynamic pressure distributions, and η_1 is the viscosity of the droplet.

The boundary conditions for the fluid velocity at the droplet surface, on the plane walls, and far removed from the droplet are

$$r = a: \quad \mathbf{e}_r\cdot(\mathbf{v} - U\mathbf{e}_x) = 0, \tag{4a}$$

$$\mathbf{v} = \mathbf{v}_1, \tag{4b}$$

$$(\mathbf{I} - \mathbf{e}_r\mathbf{e}_r)\mathbf{e}_r : (\boldsymbol{\tau} - \boldsymbol{\tau}_1) = \mathbf{0}, \tag{4c}$$

$$z = c, -b: \quad \mathbf{v} = \mathbf{0}, \tag{4d}$$

$$\rho \to \infty: \quad \mathbf{v} = \mathbf{0}. \tag{4e}$$

Here, $\tau = \eta[\nabla\mathbf{v} + (\nabla\mathbf{v})^{\mathrm{T}}]$ and $\tau_1 = \eta_1[\nabla\mathbf{v}_1 + (\nabla\mathbf{v}_1)^{\mathrm{T}}]$ are viscous stress tensors for the external flow and the flow inside the droplet, respectively; $\mathbf{e}_r$ together with $\mathbf{e}_\theta$ and $\mathbf{e}_\phi$ are the unit vectors in spherical coordinates; $\mathbf{I}$ is the unit dyadic.

In view of the linearity of the governing equations and boundary conditions, the external velocity field $\mathbf{v}$ can be decomposed into two contributions (Ganatos et al. 1980),

$$\mathbf{v} = \mathbf{v}_w + \mathbf{v}_s. \tag{5}$$

Here, $\mathbf{v}_w$ is a solution of Eq. (2) in rectangular coordinates that represents the disturbance produced by the plane walls and is given by

$$\mathbf{v}_w = v_{wx}\mathbf{e}_x + v_{wy}\mathbf{e}_y + v_{wz}\mathbf{e}_z, \tag{6}$$

where $\mathbf{e}_x$, $\mathbf{e}_y$, and $\mathbf{e}_z$ are the unit vectors in rectangular coordinates, and v_{wx}, v_{wy}, v_{wz} are the double Fourier

integrals,

$$v_{wx} = \int_0^\infty \int_0^\infty D_1(\alpha,\beta,z)\cos(\alpha x)\cos(\beta y)\,\mathrm{d}\alpha\,\mathrm{d}\beta, \tag{7a}$$

$$v_{wy} = \int_0^\infty \int_0^\infty D_2(\alpha,\beta,z)\sin(\alpha x)\sin(\beta y)\,\mathrm{d}\alpha\,\mathrm{d}\beta, \tag{7b}$$

$$v_{wz} = \int_0^\infty \int_0^\infty D_3(\alpha,\beta,z)\sin(\alpha x)\cos(\beta y)\,\mathrm{d}\alpha\,\mathrm{d}\beta. \tag{7c}$$

In Eq. (7),

$$D_1 = \left[X^*\left(1+\frac{\alpha^2}{\kappa}z\right) - X^{**}\frac{\alpha\beta}{\kappa}z - X^{***}\alpha z\right]\mathrm{e}^{\kappa z} + \left[Y^*\left(1-\frac{\alpha^2}{\kappa}z\right) + Y^{**}\frac{\alpha\beta}{\kappa}z - Y^{***}\alpha z\right]\mathrm{e}^{-\kappa z}, \tag{8a}$$

$$D_2 = \left[-X^*\frac{\alpha\beta}{\kappa}z + X^{**}\left(1+\frac{\beta^2}{\kappa}z\right) + X^{***}\beta z\right]\mathrm{e}^{\kappa z} + \left[Y^*\frac{\alpha\beta}{\kappa}z + Y^{**}\left(1-\frac{\beta^2}{\kappa}z\right) + Y^{***}\beta z\right]\mathrm{e}^{-\kappa z}, \tag{8b}$$

$$D_3 = [X^*\alpha z - X^{**}\beta z + X^{***}(1-\kappa z)]\mathrm{e}^{\kappa z} + [Y^*\alpha z - Y^{**}\beta z + Y^{***}(1+\kappa z)]\mathrm{e}^{-\kappa z}, \tag{8c}$$

where the starred X and Y are unknown functions of separation variables α and β, and $\kappa^2 = \alpha^2 + \beta^2$.

The second part of $\mathbf{v}$ in Eq. (5), denoted by $\mathbf{v}_s$, is a solution of Eq. (2) in spherical coordinates representing the disturbance generated by the droplet and is given by

$$\mathbf{v}_s = v_{sx}\mathbf{e}_x + v_{sy}\mathbf{e}_y + v_{sz}\mathbf{e}_z, \tag{9}$$

where

$$v_{sx} = \sum_{n=1}^\infty (A_nA_n' + B_nB_n' + C_nC_n'), \tag{10a}$$

$$v_{sy} = \sum_{n=1}^\infty (A_nA_n'' + B_nB_n'' + C_nC_n''), \tag{10b}$$

$$v_{sz} = \sum_{n=1}^\infty (A_nA_n''' + B_nB_n''' + C_nC_n'''). \tag{10c}$$

In Eq. (10), the primed A_n, B_n, and C_n are functions of position involving associated Legendre functions of $\cos\theta$ defined in the appendix, which were also given by Eq. (2.6) of Ganatos et al. (1980), and A_n, B_n, and C_n are unknown constants. Note that the boundary condition in Eq. (4e) is immediately satisfied by a solution of the form given by Eqs. (5)–(10).

The solution to Eq. (3) for the internal velocity field can be expressed as

$$\mathbf{v}_1 = v_{1r}\mathbf{e}_r + v_{1\theta}\mathbf{e}_\theta + v_{1\phi}\mathbf{e}_\phi, \tag{11}$$

where

$$v_{1r} = \sum_{n=1}^\infty nP_n^1(\mu)(\bar{C}_n r^{n-1} + \bar{A}_n r^{n+1})\cos\phi, \tag{12a}$$

$$v_{1\theta} = \sum_{n=1}^\infty \left[\bar{B}_n r^n P_n^1(\mu)(1-\mu^2)^{-1/2} - (1-\mu^2)^{1/2}\frac{\mathrm{d}P_n^1(\mu)}{\mathrm{d}\mu} \times \left(\bar{C}_n r^{n-1} - \bar{A}_n\frac{n+3}{n+1}r^{n+1}\right)\right]\cos\phi, \tag{12b}$$

$$v_{1\phi} = \sum_{n=1}^\infty \left[\bar{B}_n r^n (1-\mu^2)^{1/2}\frac{\mathrm{d}P_n^1(\mu)}{\mathrm{d}\mu} - (1-\mu^2)^{-1/2}P_n^1(\mu) \times \left(\bar{C}_n r^{n-1} - \bar{A}_n\frac{n+3}{n+1}r^{n+1}\right)\right]\sin\phi, \tag{12c}$$

P_n^m is the associated Legendre function of order n and degree m, μ is used to denote $\cos\theta$ for brevity, and $\bar{A}_n, \bar{B}_n$, and $\bar{C}_n$ are unknown constants. A solution of this form satisfies the requirement that the velocity is finite for any position within the droplet. Note that the solution for $\mathbf{v}_1$ contains only terms of $\cos\phi$ and $\sin\phi$ (and not higher-order harmonics) due to the symmetry of the geometry of the system.

A brief conceptual description of the solution procedure to determine the starred X and Y functions in Eq. (8) and the constants $A_n, B_n, C_n, \bar{A}_n, \bar{B}_n$, and $\bar{C}_n$ in Eqs. (10) and (12) is given below to help follow the mathematical development. At first, boundary conditions [given by Eq. (4d)] are exactly satisfied on the plane walls by using the Fourier transforms. This permits the unknown starred X and Y functions to be determined in terms of the coefficients A_n, B_n, and C_n. Then, the boundary conditions in Eqs. (4a)–(4c) on the surface of the droplet can be satisfied by making use of the collocation method, and the solution of the collocation matrix provides numerical values for the coefficients $A_n, B_n, C_n, \bar{A}_n, \bar{B}_n$, and $\bar{C}_n$.

Substitution of the velocity distribution $\mathbf{v}$ given by Eqs. (5)–(10) into the boundary conditions of Eq. (4d) and application of the Fourier sine and cosine inversions on the variables x and y, respectively, lead to a solution for the functions D_1, D_2, and D_3 (or starred X and Y functions) in terms of the coefficients A_n, B_n, and C_n. After the substitution of this solution back into Eq. (7) and utilization of the integral representations of the modified Bessel functions of the second kind, the external fluid velocity field can be expressed as

$$\mathbf{v} = v_x\mathbf{e}_x + v_y\mathbf{e}_y + v_z\mathbf{e}_z, \tag{13}$$

where

$$v_x = \sum_{n=1}^\infty [A_n(A_n' + \alpha_n') + B_n(B_n' + \beta_n') + C_n(C_n' + \gamma_n')], \tag{14a}$$

$$v_y = \sum_{n=1}^{\infty} [A_n(A_n'' + \alpha_n'') + B_n(B_n'' + \beta_n'') + C_n(C_n'' + \gamma_n'')], \tag{14b}$$

$$v_z = \sum_{n=1}^{\infty} [A_n(A_n''' + \alpha_n''') + B_n(B_n''' + \beta_n''') + C_n(C_n''' + \gamma_n''')]. \tag{14c}$$

Here, the primed α_n, β_n, and γ_n are complicated functions of position in the form of integration (which must be performed numerically) defined by Eq. (C1) of Ganatos et al. (1980).

The boundary conditions that remain to be satisfied are those on the droplet surface. Substituting Eqs. (11)–(14) into Eqs. (4a)–(4c), one obtains

$$\sum_{n=1}^{\infty} [A_n A_n^*(a,\mu,\phi) + B_n B_n^*(a,\mu,\phi) + C_n C_n^*(a,\mu,\phi)] = U_x(1-\mu^2)^{1/2}\cos\phi, \tag{15a}$$

$$\sum_{n=1}^{\infty} [A_n A_n^*(a,\mu,\phi) + B_n B_n^*(a,\mu,\phi) + C_n C_n^*(a,\mu,\phi)] - \sum_{n=1}^{\infty} [\bar{C}_n n a^{n-1} P_n^1(\mu) + \bar{A}_n n a^{n+1} P_n^1(\mu)]\cos\phi = 0, \tag{15b}$$

$$\sum_{n=1}^{\infty} [A_n A_n^{**}(a,\mu,\phi) + B_n B_n^{**}(a,\mu,\phi) + C_n C_n^{**}(a,\mu,\phi)] - \sum_{n=1}^{\infty} \left[\bar{B}_n a^n (1-\mu^2)^{-1/2} P_n^1(\mu) - \bar{C}_n a^{n-1}(1-\mu^2)^{1/2} \frac{dP_n^1}{d\mu} - \bar{A}_n \frac{n+3}{n+1} \times a^{n+1}(1-\mu^2)^{1/2} \frac{dP_n^1}{d\mu} \right] \cos\phi = 0, \tag{15c}$$

$$\sum_{n=1}^{\infty} [A_n A_n^{***}(a,\mu,\phi) + B_n B_n^{***}(a,\mu,\phi) + C_n C_n^{***}(a,\mu,\phi)] - \sum_{n=1}^{\infty} \left[\bar{B}_n a^n (1-\mu^2)^{1/2} \frac{dP_n^1}{d\mu} - \bar{C}_n a^{n-1}(1-\mu^2)^{-1/2} P_n^1(\mu) - \bar{A}_n \frac{n+3}{n+1} \times a^{n+1}(1-\mu^2)^{-1/2} P_n^1(\mu) \right] \sin\phi = 0, \tag{15d}$$

$$\sum_{n=1}^{\infty} \left\{ \left(\frac{\partial}{\partial r} - \frac{1}{r} \right) [A_n A_n^{**}(r,\mu,\phi) + B_n B_n^{**}(r,\mu,\phi) + C_n C_n^{**}(r,\mu,\phi)] - \frac{(1-\mu^2)^{1/2}}{r} \frac{\partial}{\partial \mu} [A_n A_n^*(r,\mu,\phi) + B_n B_n^*(r,\mu,\phi) + C_n C_n^*(r,\mu,\phi)] \right\}_{r=a} - \eta^* \sum_{n=1}^{\infty} \left[\bar{B}_n (n-1) a^{n-1} P_n^1(\mu)(1-\mu^2)^{-1/2} - \bar{C}_n 2(n-1) a^{n-2}(1-\mu^2)^{1/2} \frac{dP_n^1(\mu)}{d\mu} - \bar{A}_n \frac{n(n+2)}{n+1} a^n (1-\mu^2)^{1/2} \frac{dP_n^1(\mu)}{d\mu} \right] \cos\phi = 0, \tag{15e}$$

$$\sum_{n=1}^{\infty} \left\{ \left(\frac{\partial}{\partial r} - \frac{1}{r} \right) [A_n A_n^{***}(r,\mu,\phi) + B_n B_n^{***}(r,\mu,\phi) + C_n C_n^{***}(r,\mu,\phi)] + \frac{(1-\mu^2)^{-1/2}}{r} \frac{\partial}{\partial \phi} [A_n A_n^*(r,\mu,\phi) + B_n B_n^*(r,\mu,\phi) + C_n C_n^*(r,\mu,\phi)] \right\}_{r=a} - \eta^* \sum_{n=1}^{\infty} \left[\bar{B}_n (n-1) a^{n-1} (1-\mu^2)^{1/2} \frac{dP_n^1(\mu)}{d\mu} - \bar{C}_n 2(n-1) a^{n-2}(1-\mu^2)^{-1/2} P_n^1(\mu) - \bar{A}_n \frac{n(n+2)}{n+1} a^n (1-\mu^2)^{-1/2} P_n^1(\mu) \right] \sin\phi = 0, \tag{15f}$$

where $\eta^* = \eta_1/\eta$. The starred A_n, B_n, and C_n functions in Eq. (15) are defined by

$$A_n^*(r,\mu,\phi) = (1-\mu^2)^{1/2}(A_n' + \alpha_n')\cos\phi + (1-\mu^2)^{1/2}(A_n'' + \alpha_n'')\sin\phi + \mu(A_n''' + \alpha_n'''), \tag{16a}$$

$$B_n^*(r,\mu,\phi) = (1-\mu^2)^{1/2}(B_n' + \beta_n')\cos\phi + (1-\mu^2)^{1/2} \times (B_n'' + \beta_n'')\sin\phi + \mu(B_n''' + \beta_n'''), \tag{16b}$$

$$C_n^*(r,\mu,\phi) = (1-\mu^2)^{1/2}(C_n' + \gamma_n')\cos\phi + (1-\mu^2)^{1/2} \times (C_n'' + \gamma_n'')\sin\phi + \mu(C_n''' + \gamma_n'''), \tag{16c}$$

$$A_n^{**}(r,\mu,\phi) = \mu(A_n' + \alpha_n')\cos\phi + \mu(A_n'' + \alpha_n'')\sin\phi - (1-\mu^2)^{1/2}(A_n''' + \alpha_n'''), \quad (16d)$$

$$B_n^{**}(r,\mu,\phi) = \mu(B_n' + \beta_n')\cos\phi + \mu(B_n'' + \beta_n'')\sin\phi - (1-\mu^2)^{1/2}(B_n''' + \beta_n'''), \quad (16e)$$

$$C_n^{**}(r,\mu,\phi) = \mu(C_n' + \gamma_n')\cos\phi + \mu(C_n'' + \gamma_n'')\sin\phi - (1-\mu^2)^{1/2}(C_n''' + \gamma_n'''), \quad (16f)$$

$$A_n^{***}(r,\mu,\phi) = -(A_n' + \alpha_n')\sin\phi + (A_n'' + \alpha_n'')\cos\phi, \quad (16g)$$

$$B_n^{***}(r,\mu,\phi) = -(B_n' + \beta_n')\sin\phi + (B_n'' + \beta_n'')\cos\phi, \quad (16h)$$

$$C_n^{***}(r,\mu,\phi) = -(C_n' + \gamma_n')\sin\phi + (C_n'' + \gamma_n'')\cos\phi, \quad (16i)$$

where the primed $A_n, B_n, C_n, \alpha_n, \beta_n$, and γ_n are functions of position in Eqs. (10) and (14).

Careful examination of Eq. (15) shows that the solution of the coefficient matrix generated is independent of the ϕ coordinate of the boundary points on the spherical surface $r = a$. To satisfy the conditions in Eq. (15) exactly along the entire surface of the droplet would require the solution of the entire infinite array of unknown constants $A_n, B_n, C_n, \bar{A}_n$, $\bar{B}_n$, and $\bar{C}_n$. However, the collocation technique (O'Brien, 1968; Ganatos et al., 1980; Keh & Tseng, 1992; Chen & Ye, 2000) enforces the boundary conditions at a finite number of discrete points on the half-circular generating arc of the droplet (from $\theta = 0$ to π) and truncates the infinite series in Eqs. (12) and (14) into finite ones. If the spherical boundary is approximated by satisfying the conditions of Eqs. (4a)–(4c) at N discrete points on its generating arc, the infinite series in Eqs. (12) and (14) are truncated after N terms, resulting in a system of $6N$ simultaneous linear algebraic equations in the truncated form of Eq. (15). This matrix equation can be solved to yield the $6N$ unknown constants $A_n, B_n, C_n, \bar{A}_n, \bar{B}_n$, and $\bar{C}_n$ appearing in the truncated form of Eqs. (12) and (14). The fluid velocity field is completely obtained once these coefficients are solved. Note that the definite integrals in Eq. (15) after the substitution of Eq. (16) must be performed numerically. The accuracy of the truncation technique can be improved to any degree by taking a sufficiently large value of N. Naturally, as $N \to \infty$ the truncation error vanishes and the overall accuracy of the solution depends only upon the numerical integration required in evaluating the matrix elements.

The drag force exerted by the external fluid on the spherical droplet can be determined from (Ganatos et al., 1980)

$$\mathbf{F} = -8\pi\eta A_1 \mathbf{e}_x. \quad (17)$$

This expression shows that only the lowest-order coefficient A_1 contributes to the hydrodynamic force acting on the droplet.

3. Results and discussion

The solution for the slow motion of a spherical droplet parallel to two plane walls at an arbitrary position between them, obtained by using the boundary collocation technique described in the previous section, will be presented in this section. The system of linear algebraic equations to be solved for coefficients $A_n, B_n, C_n, \bar{A}_n, \bar{B}_n$, and $\bar{C}_n$ is constructed from Eq. (15). All the numerical integrations to evaluate the starred A_n, B_n, and C_n functions (or the primed α_n, β_n, and γ_n functions) were done by the 40-point Gauss–Laguerre quadrature. The numerical calculations were performed by using a DEC 3000/600 workstation.

When specifying the points along the semicircular generating arc of the sphere where the boundary conditions are to be exactly satisfied, the first points that should be chosen are $\theta = 0$ and π, since these points define the projected area of the droplet normal to the direction of motion and control the gaps between the droplet and the neighboring walls. In addition, the point $\theta = \pi/2$ is also important. However, an examination of the system of linear algebraic equations in Eq. (15) shows that this matrix equation becomes singular if these points are used. To overcome this difficulty, these points are replaced by closely adjacent points, i.e., $\theta = \delta, \pi/2 - \delta, \pi/2 + \delta$, and $\pi - \delta$. Additional points along the boundary are selected as mirror-image pairs about the plane $\theta = \pi/2$ to divide the two quarter-circular arcs of the droplet into equal segments. The optimum value of δ in this work is found to be 0.1°, with which the numerical results of the hydrodynamic drag force acting on the droplet converge satisfactorily. In selecting the boundary points, any value of ϕ may be used except $\phi = 0$, $\pi/2$, and π, since the matrix equation (15) is singular for these values.

The collocation solutions of the hydrodynamic drag force exerted on a fluid droplet translating parallel to a single plane wall (with $c \to \infty$) for various values of a/b and η^* are presented in Table 1. The drag force F_0 acting on an identical droplet in an unbounded fluid, given by Eq. (1) (with $\mathbf{F}_0 = F_0\mathbf{e}_x$), is used to normalize the boundary-corrected values. Obviously, $F/F_0 = 1$ as $a/b = 0$ for any value of η^*. The accuracy and convergence behavior of the truncation technique depends principally upon the ratio a/b. All of the results obtained under this collocation scheme converge to at least five significant figures. For the difficult case of $a/b = 0.999$ the number of collocation points $N = 36$ is sufficiently large to achieve this convergence. For the special case of translation of a rigid sphere (with $\eta^* \to \infty$) parallel to a plane wall, our numerical results agree perfectly with the semi-analytical solution obtained using

Table 1
The normalized drag force F/F_0 experienced by a spherical droplet translating parallel to a single plane wall at various values of a/b and η^*

a/b	F/F_0			
	$\eta^*=0$	$\eta^*=1$	$\eta^*=10$	$\eta^*=\infty$
0.1	1.0390	1.0491	1.0576	1.0595
0.2	1.0812	1.1030	1.1217	1.1259
0.3	1.1273	1.1625	1.1932	1.2003
0.4	1.1783	1.2288	1.2741	1.2847
0.5	1.2358	1.3040	1.3675	1.3828
0.6	1.3028	1.3918	1.4790	1.5006
0.7	1.3847	1.4988	1.6191	1.6503
0.8	1.4948	1.6399	1.8109	1.8591
0.9	1.6776	1.8601	2.1262	2.2152
0.95	1.8620	2.0610	2.4255	2.5725
0.975	2.0425	2.2417	2.6978	2.9225
0.99	2.2324	2.4236	2.9759	3.3347
0.995	2.3205	2.5080	3.1100	3.5821
0.999	2.4030	2.5883	3.2439	3.9048

spherical bipolar coordinates (O'Neill, 1964; Goldman, Cox, and Brenner, 1967). As expected, the results in Table 1 illustrate that the drag force on the droplet is a monotonically increasing function of a/b, and will become infinite in the limit $a/b=1$, for any given value of η^*. Also, the wall-corrected normalized drag force on the droplet increases monotonically with an increase in η^*, keeping a/b unchanged.

A number of converged numerical solutions for the normalized drag force F/F_0 are presented in Table 2 for the translation of a spherical droplet parallel to two plane walls at two particular positions between them (with $b/(b+c)=0.25$ and 0.5) for various values of a/b and η^* using the boundary collocation technique. For the special case of a rigid sphere (with $\eta^* \to \infty$), our results agree well with the previous solution obtained by a similar collocation method (Ganatos et al., 1980), in which no tabulated values are available for a precise comparison). Using a method of reflections, Shapira and Haber (1988) obtained a formula for the drag force acting on a droplet of arbitrary viscosity translating parallel to two plates to the first order of $a/(b+c)$. The values of the wall-corrected drag force calculated from this approximate formula are also listed in Table 2 for comparison. It can be seen that the method-of-reflection solution to the leading order agrees with the exact solution for

Table 2
The normalized drag force F/F_0 experienced by a spherical droplet translating parallel to two plane walls at various values of a/b, s $(=b/(b+c))$, and η^*[a]

s	a/b	F/F_0			
		$\eta^*=0$	$\eta^*=1$	$\eta^*=10$	$\eta^*=\infty$
0.25	0.1	1.0455 (1.0435)	1.0574 (1.0544)	1.0674 (1.0633)	1.0697 (1.0653)
	0.2	1.0954 (1.0870)	1.1215 (1.1088)	1.1438 (1.1266)	1.1489 (1.1306)
	0.3	1.1505 (1.1305)	1.1931 (1.1632)	1.2304 (1.1899)	1.2391 (1.1958)
	0.4	1.2121 (1.1740)	1.2737 (1.2175)	1.3295 (1.2531)	1.3427 (1.2611)
	0.5	1.2821 (1.2175)	1.3657 (1.2719)	1.4445 (1.3164)	1.4635 (1.3263)
	0.6	1.3637 (1.2611)	1.4730 (1.3263)	1.5812 (1.3797)	1.6080 (1.3916)
	0.7	1.4628 (1.3046)	1.6024 (1.3807)	1.7504 (1.4430)	1.7884 (1.4568)
	0.8	1.5931 (1.3481)	1.7689 (1.4351)	1.9756 (1.5063)	2.0322 (1.5221)
	0.9	1.8000 (1.3916)	2.0178 (1.4895)	2.3294 (1.5696)	2.4278 (1.5874)
	0.95	1.9979	2.2342	2.6501	2.8067
	0.975	2.1858	2.4227	2.9337	3.1677
	0.99	2.3802	2.6093	3.2192	3.5870
	0.995	2.4699	2.6952	3.3562	3.8367
	0.999	2.5536	2.7767	3.4926	4.1613
0.5	0.1	1.0717 (1.0669)	1.0911 (1.0837)	1.1074 (1.0974)	1.1111 (1.1004)
	0.2	1.1546 (1.1339)	1.1986 (1.1674)	1.2373 (1.1947)	1.2462 (1.2008)
	0.3	1.2513 (1.2008)	1.3256 (1.2510)	1.3935 (1.2921)	1.4096 (1.3012)
	0.4	1.3659 (1.2678)	1.4758 (1.3347)	1.5812 (1.3895)	1.6068 (1.4016)
	0.5	1.5040 (1.3347)	1.6547 (1.4184)	1.8074 (1.4868)	1.8458 (1.5021)
	0.6	1.6748 (1.4016)	1.8709 (1.5021)	2.0840 (1.5842)	2.1395 (1.6025)
	0.7	1.8939 (1.4686)	2.1340 (1.5857)	2.4324 (1.6816)	2.5124 (1.7029)
	0.8	2.1939 (1.5355)	2.4925 (1.6694)	2.9001 (1.7790)	3.0194 (1.8033)
	0.9	2.6733 (1.6025)	3.0239 (1.7531)	3.6336 (1.8763)	3.8369 (1.9037)
	0.95	3.1154	3.4801	4.2925	4.6101
	0.975	3.5181	3.8711	4.8709	5.3405
	0.99	3.9244	4.2535	5.4513	6.1841
	0.995	4.1096	4.4287	5.7303	6.6854
	0.999	4.2818	4.5942	6.0090	7.3358

[a]The values in parentheses are calculated from the approximate formula obtained by Shapira and Haber (1988) using the method of reflections.

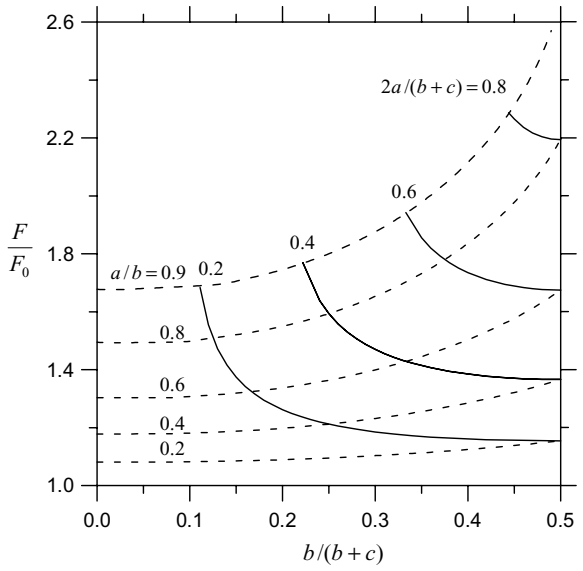

Fig. 2. Plots of the normalized drag force F/F_0 on a spherical gas bubble (with $\eta^* \to 0$) translating parallel to two plane walls versus the ratio $b/(b+c)$ with a/b and $2a/(b+c)$ as parameters.

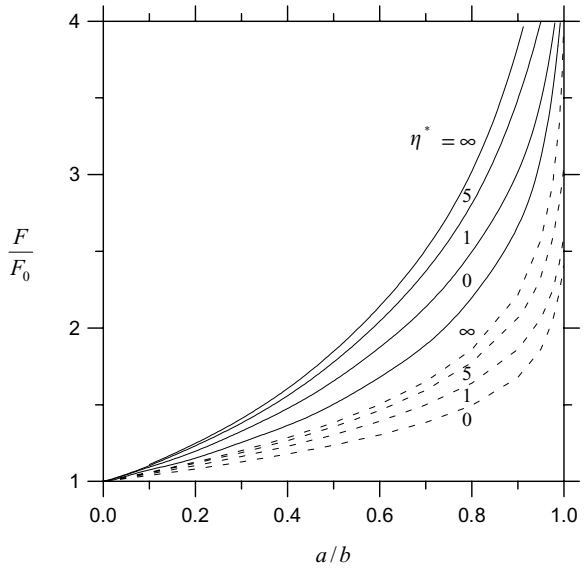

Fig. 3. Plots of the normalized drag force F/F_0 on a spherical droplet translating on the midplane between two parallel plane walls (with $c=b$) versus the ratio a/b with η^* as a parameter. The dashed curves are plotted for the translation of an identical droplet parallel to a single plane wall for comparison.

small values of a/b. The errors are less than 3.7% for cases with $a/b \leqslant 0.2$. However, the accuracy of this approximate solution begins to deteriorate, as expected, when the droplet gets closer to the walls. For example, the errors can be greater than 12% for cases with $a/b=0.4$. Analogous to the situation of translation parallel to a single wall, for a constant value of $b/(b+c)$, Table 2 indicates that the normalized drag force on the droplet increases monotonically with an increase in a/b (again, $F/F_0=1$ as $a/b=0$) for a fixed value of η^* and with an increase in η^* for a given value of a/b.

Fig. 2 shows the drag force exerted on a gas bubble (with $\eta^* \to 0$) translating parallel to two plane walls. The dashed curves (with $a/b=$ constant) illustrate the effect of the position of the second wall (at $z=c$) on the drag for various values of the sphere-to-wall spacing b/a. The solid curves (with $2a/(b+c)=$ constant) indicate the variation of the drag force as a function of the sphere position at various values of the wall-to-wall spacing $(b+c)/2a$. At a given value of $2a/(b+c)$, the bubble (or a droplet with a finite value of η^*, whose result is not exhibited here but can also be obtained accurately) experiences minimum drag when it is located midway between the two walls, analogous to the corresponding case of a solid sphere (Ganatos et al., 1980). The drag force becomes infinite as the bubble (or a droplet with finite η^*) approaches either of the walls.

In Fig. 3, the normalized drag force on a spherical droplet translating on the midplane between two parallel plane walls (with $c=b$) is plotted by solid curves as a function of a/b for various values of η^*. The corresponding drag on the droplet when the second wall is not present (with $c \to \infty$) is also plotted by dashed curves in the same figure for comparison. It can be seen from this figure (or from a comparison between Tables 1 and 2) that, for an arbitrary combination of parameters a/b and η^*, the assumption that the results for two walls can be obtained by simple addition of the single-wall effect gives too large a correction to the hydrodynamic drag on a droplet if a/b is small (say, < 0.25) but underestimates the wall correction if a/b is relatively large (say, > 0.35).

4. Concluding remarks

In this work the slow motion of a spherical droplet parallel to two plane walls at an arbitrary position between them is studied theoretically. A semi-analytical method with the boundary collocation technique has been used to solve the Stokes equations for the velocity fields in the fluid phases. The results for the hydrodynamic drag force exerted on the droplet indicate that the solution procedure converges rapidly and accurate solutions can be obtained for various cases of the relative viscosity of the droplet and the separation between the droplet and the walls. It has been found that, for a given relative position of the walls, the wall-corrected drag acting on the droplet normalized by the value in the absence of the walls is a monotonically increasing function of the ratio of viscosity between the internal and surrounding fluids. For a given droplet translating between two parallel walls separated by a fixed distance, the droplet experiences minimum drag when it is located midway between the walls, and

the drag becomes infinite as the droplet touches either of the walls.

In Tables 1 and 2 as well as Figs. 2 and 3, we presented only the results for resistance problems, defined as those in which the drag force F acting on the droplet is to be determined for a specified droplet velocity $U[=-(F_0/6\pi\eta a)(3\eta^*+3)/(3\eta^*+2)]$. In a mobility problem, on the other hand, the applied force $F[=6\pi\eta a U_0(3\eta^*+2)/(3\eta^*+3)]$ exerted on the droplet is specified and the droplet velocity U is to be determined. For the creeping motion of a spherical droplet with a finite viscosity located between two parallel planes considered in this work, the ratio U/U_0 for a mobility problem equals the ratio $(F/F_0)^{-1}$ for its corresponding resistance problem. Thus, our results can also be applied to physical problems in which the force on the droplet is the prescribed quantity and the droplet must move accordingly.

Notation

a	radius of the droplet, m
A_n, B_n, C_n	coefficients in the expression of Eq. (10) for the external flow field, $m^{n+1}\ s^{-1}$, $m^{n+3}\ s^{-1}$, $m^{n+2}\ s^{-1}$
$\bar{A}_n, \bar{B}_n, \bar{C}_n$	coefficients in the expression of Eq. (12) for the internal flow field, $m^{-n}\ s^{-1}$, $m^{-n+1}\ s^{-1}$, $m^{-n+2}\ s^{-1}$
A'_n, B'_n, C'_n A''_n, B''_n, C''_n A'''_n, B'''_n, C'''_n	functions of position defined by Eqs. (A.1)–(A.9), m^{-n}, m^{-n-2}, m^{-n-1}
b, c	the respective distances from the droplet center to the two plates, m
$\mathbf{e}_x, \mathbf{e}_y, \mathbf{e}_z$	unit vectors in rectangular coordinates
$\mathbf{e}_r, \mathbf{e}_\theta, \mathbf{e}_\phi$	unit vectors in spherical coordinates
$\mathbf{F}, F$	drag force acting on the droplet, N
$\mathbf{F}_0, F_0$	drag force acting on the droplet in an unbounded fluid, N
N	number of collocation points on the droplet surface
P_n^m	associated Legendre function of order n and degree m
r	radial spherical coordinate, m
$\mathbf{U}, U$	translational velocity of the droplet, m s^{-1}
$\mathbf{v}$	velocity field of the external fluid, m s^{-1}
$\mathbf{v}_1$	fluid velocity field inside the droplet, m s^{-1}
x, y, z	rectangular coordinates, m

Greek letters

$\alpha'_n, \beta'_n, \gamma'_n$, $\alpha''_n, \beta''_n, \gamma''_n$ $\alpha'''_n, \beta'''_n, \gamma'''_n$	functions of position defined by Eq. (C1) of Ganatos et al. (1980), m^{-n}, m^{-n-2}, m^{-n-1}
η	viscosity of the external fluid, kg $m^{-1}\ s^{-1}$
η_1	viscosity of the fluid inside the droplet, kg $m^{-1}\ s^{-1}$
η^*	$=\eta_1/\eta$
θ, ϕ	angular spherical coordinates
μ	$=\cos\theta$
ρ	radial cylindrical coordinate, m

Acknowledgements

Part of this research was supported by the National Science Council of the Republic of China.

Appendix

For the sake of completion, the definitions of the primed A_n, B_n, and C_n functions in Eq. (10) are given here.

$$A'_n = \frac{1}{2r^n}[2n(2n-1)(1-\mu^2)^{1/2}P_n^1(\mu)\cos^2\phi + (n-2)P_{n-1}^2(\mu)\cos 2\phi - n(n+1)(n-2)P_{n-1}(\mu)], \tag{A.1}$$

$$B'_n = -\frac{1}{2r^{n+2}}[P_{n+1}^2(\mu)\cos 2\phi - n(n+1)P_{n+1}(\mu)], \tag{A.2}$$

$$C'_n = \frac{1}{2r^{n+1}}[P_n^2(\mu)\cos 2\phi + n(n+1)P_n(\mu)], \tag{A.3}$$

$$A''_n = \frac{1}{r^n}[n(2n-1)(1-\mu^2)^{1/2}P_n^1(\mu) + (n-2)P_{n-1}^2(\mu)]\cos\phi\sin\phi, \tag{A.4}$$

$$B''_n = -\frac{1}{r^{n+2}}P_{n+1}^2(\mu)\cos\phi\, sin\,\phi, \tag{A.5}$$

$$C''_n = \frac{1}{r^{n+1}}P_n^2(\mu)\cos\phi\sin\phi, \tag{A.6}$$

$$A'''_n = \frac{1}{r^n}[n(2n-1)\mu P_n^1(\mu) - (n+1)(n-2)P_{n-1}^1(\mu)]\cos\phi, \tag{A.7}$$

$$B'''_n = -\frac{1}{r^{n+2}}nP_{n+1}^1(\mu)\cos\phi, \tag{A.8}$$

$$C'''_n = -\frac{1}{r^{n+1}}P_n^1(\mu)\cos\phi. \tag{A.9}$$

References

Bart, E. (1968). The slow unsteady settling of a fluid sphere toward a flat fluid interface. *Chemical Engineering Science*, *23*, 193–210.

Brenner, H. (1961). The slow motion of a sphere through a viscous fluid towards a plane surface. *Chemical Engineering Science*, *16*, 242–251.

Brenner, H. (1971). Pressure drop due to the motion of neutrally buoyant particles in duct flows. II. Spherical droplets and bubbles. *Industrial and Engineering Chemistry Fundamentals*, *10*, 537–542.

Chen, S. B., & Ye, X. (2000). Boundary effect on slow motion of a composite sphere perpendicular to two parallel impermeable plates. *Chemical Engineering Science*, *55*, 2441–2453.

Coutanceau, M., & Thizon, P. (1981). Wall effect on the bubble behaviour in highly viscous liquids. *Journal of Fluid Mechanics*, *107*, 339–373.

Dandy, D. S., & Leal, L. G. (1989). Bouyancy-driven motion of a deformable drop through a quiescent liquid at intermediate Reynolds numbers. *Journal of Fluid Mechanics*, *208*, 161–192.

Ganatos, P., Pfeffer, R., & Weinbaum, S. (1980). A strong interaction theory for the creeping motion of a sphere between plane parallel boundaries. Part 2. Parallel motion. *Journal of Fluid Mechanics*, *99*, 755–783.

Goldman, A. J., Cox, R. G., & Brenner, H. (1967). Slow viscous motion of a sphere parallel to a plane wall-I. Motion through a quiescent fluid. *Chemical Engineering Science*, *22*, 637–651.

Hadamard, J. S. (1911). Movement permanent lent d'une sphere liquide et visqueuse dans un liquide visqueux. *Comptes Rendus Hebdomadaires des Seances de V Academie des Sciences (Paris)*, *152*, 1735–1738.

Hetsroni, G., Haber, S., & Wacholder, E. (1970). The flow fields in and around a droplet moving axially within a tube. *Journal of Fluid Mechanics*, *41*, 689–705.

Keh, H. J., & Tseng, Y. K. (1992). Slow motion of multiple droplets in arbitrary three-dimensional configurations. *A.I.Ch.E. Journal*, *38*, 1881–1904.

Maude, A. D. (1961). End effects in a falling-sphere viscometer. *Britain Journal of Applied Physics*, *12*, 293–295.

O'Brien, V. (1968). Form factors for deformed spheroids in Stokes flow. *A.I.Ch.E. Journal*, *14*, 870–875.

O'Neill, M. E. (1964). A slow motion of viscous liquid caused by a slowly moving solid sphere. *Mathematika*, *11*, 67–74.

Rushton, E., & Davies, G. A. (1973). The slow unsteady settling of two fluid spheres along their line of centres. *Applied Scientific Research*, *28*, 37–61.

Rybczynski, W. (1911). Uber die Fortschreitende Bewegung einer flussigen Kugel in einem zahen Medium. *Bull. Acad. Sci. Cracovie Ser. A*, *1*, 40–46.

Shapira, M., & Haber, S. (1988). Low Reynolds number motion of a droplet between two parallel plates. *International Journal of Multiphase Flow*, *14*, 483–506.

Taylor, T. D., & Acrivos, A. (1964). On the deformation and drag of a falling viscous drop at low Reynolds number. *Journal of Fluid Mechanics*, *18*, 466–476.

Wacholder, E., & Weihs, D. (1972). Slow motion of a fluid sphere in the vicinity of another sphere or a plane boundary. *Chemical Engineering Science*, *27*, 1817–1828.